Non-Destructive Resonance Testing

Using Frequency and Time Domain Techniques

by

Osama Jameel

A Thesis Presented in Partial Fulfillment
of the Requirements for the Degree
Master of Science in Technology

Approved October 2013 by the
Graduate Supervisory Committee:

Sangram Redkar, Chair
Sharon Lewis
Robert Meitz

ARIZONA STATE UNIVERSITY

December 2013

ABSTRACT

The objective of this thesis is to compare various approaches for classification of the defective and non-defective parts via non-destructive resonance testing methods by collecting and analyzing experimental data in the frequency and time domains. A Laser Scanning Vibrometer was employed to measure vibrating samples in order to determine the spectral characteristics such as natural frequencies and amplitudes. Statistical pattern recognition tools such as Hilbert Huang, Fisher's Discriminant, and Neural Network were used to identify and classify the unknown samples whether they are defective or not. In this work, a Finite Element Analysis software packages (ANSYS 13.0 and NASTRAN NX8.0) was used to obtain estimates of resonance frequencies in 'good' and 'bad' samples. Furthermore, a system identification approach was used to generate Auto-Regressive-Moving Average with exogenous component, Box-Jenkins, and Output Error models from experimental data that can be used for classification.

DEDICATION

I dedicate this thesis to my committee chair, Dr. Sangram Redkar for his support and encouragement, and my parents, Mr. Mahmood Jameel and Mrs. Naeemah Kadhim. For their love and best wishes.

ACKNOWLEDGMENTS

I would like to express my deepest gratitude and appreciations to my adviser and committee chair, Dr. Sangram Redkar for his support, guidance during this journey, and for teaching me the foundations of Non-Destructive testing and vibrations analysis. I would like to acknowledge and thank Dr. Sharon Lewis for her help, support, and motivation during my courses and thesis. I would also like to thank Dr. Robert Meitz for providing me with great feedback and suggestions for my thesis.

Special appreciations and thanks to my great friends Alvaro Vargas-Clara, Pooja Velaskar, and Dipika Subramanian for their unlimited support, encouragement, and contribution in my thesis. Finally, I would like to thank my family for their love, support, and caring throughout my life.

TABLE OF CONTENTS

LIST OF TABLES

LIST OF FIGURES

Chapter 1

INTRODUCTION

1.1 Thesis Background

Resonance testing is a method of Non-Destructive Testing (NDT). It can be used to

detect defects and flaws; such as cracks and voids in parts. Each product, with specific

dimensions and material properties, has its own resonant frequencies, but these

frequencies change in the presence of defects. These defects cause a difference in the

vibrational behavior (and the natural/resonant frequencies) due to the change in the

stiffness of the part. The change and variation in stiffness between the non-defective and

defective parts cause changes in the natural frequencies; under dynamical load, they

behave differently.

  Traditional 'destructive' testing methods may include destroying some samples by

applying loads that are similar to the extreme working conditions in order to ensure the

safety and performance of the product while it is in service, these methods are called

destructive testing methods. Some of the disadvantages of destructive testing are high

cost due to the damaged parts, longer testing time, and the inability to test all the parts.

On the other hand, the testing method that do not require destroying any parts are called

NDT.   The purpose of these methods is to identify and measure abnormal conditions,

especially microscopic defects and flaws, and to do so without deforming or destroying

the part (Price, Dalley, McCullough, & Choquette, 1997). These methods are quite

common in industry. Each NDT method has some advantages and disadvantages. The

simplest method is 'visual inspection'. It is cheap and easy to perform, but it is incapable

1

of detecting internal defects. Some NDT methods require advanced technologies such as X-rays, and laser which leads to expensive testing and requiring well-trained inspectors. Testing is very important process in quality control; it is normally done at the final stages of production to make sure that the products are qualified for performing the required function before they get shipped to the costumer. Resonance testing provides important information that can be used to identify good vs. bad parts.

In this work, an electro-dynamic shaker is used to excite the part and a Laser Scanning Vibrometer is employed for gathering vibration data. This instrument uses holographic interferometry which measures velocity and displacement of light wave; it has been used in many applications such as automotive, aerospace, and biomedical (Santulli & Jeronimidis, 2006). The advantages of using the Laser Vibrometer are the accuracy, speed and no need for a physical contact with the part under test. The process consists of a laser beam being directed at a product and by generating a mesh, the beam moves through all the nodes of the mesh to complete the scan over all the points. Then the data is collected at each point which can be in frequency or time domain. In the frequency domain, the response is represented with respect to the frequency, while in the time domain varies over time. The frequency and time domain are used in the system identification tool box in MATLAB, which is a powerful tool that can be used to create a model of a system by using the response data. The time domain data of good parts can also be used to estimate the model.

In addition to system identification approach, pattern recognition methods can be employed to recognize the good and bad parts. One of the methods is Hilber Huang Transform (HHT). In this method, the non-linear non-stationary signal is decomposed

into nine harmonic signals then the frequency spectrum is evaluated from the extracted time domain data. Another method used in this work is Fisher discriminant analysis, in which good and bad frequency data are projected onto a line and then the difference between the projected means shows the variations between the good and bad samples. In addition, the neural network method is also employed for classification.

1.2 Resonance Testing Using Laser Scanning Vibrometer

Resonance testing has many advantages that make it efficient and beneficial to industry more than other methods of testing; especially when the tests are performed by an accurate powerful instrument such as the Laser Vibrometer. These advantages are:

1. The high accuracy of Laser Vibrometer allows for accurate testing results, and the velocity and displacement data can be collected which makes it easy to analyze.

2. A mesh of small elements connected by nodes can be generated to ensure that the 'automated multipoint' test can be performed at each small segment of the part to be tested.

3. This NDT method is fast and it can be used in a large product's inspection line.

4. The high frequency range helps define small and large defects.

5. No contact is required with the part under investigation. This property helps performing the test from distance or for complex geometry design products.

1.3 Problem Statement

This thesis concentrates on identifying the defects and flaws in the products and machine parts using resonance NDT methods in both frequency and time domains by employing laser vibrometry scanning technology. It also includes a comparison between defective and non-defective test samples by analyzing the data from experiments. Furthermore, an

ideal theoretical analyses are used by employing numerical software packages ANSYS and NASTRAN NX8.0.

The objectives of the thesis are accomplished by:

1. Describing the difference between frequency and time domains and explaining the fundamental operating principles of the Vibrometer.

2. Performing the experiments using the laser scanning Vibrometer and electro-dynamic shaker.

3. Applying different types of vibrational waves such as burst chirp, white noise, and sinusoidal sweep waves, then comparing the results of their response.

4. Generating mathematical models using time domain data for the part under investigation using MATLAB system identification tool box.

5. Identifying Defective and non-Defective parts, analyzing the experimental results, using frequency domain data.

6. Generating a finite element simulation using ANSYS NASTRAN NX8.0 software packages for both the defective and non-defective parts

7. Using pattern recognition tools such as neural network, Fisher's discriminant analysis, and Hilbert Huang Transform to classify the experimental data.

Chapter 2

LITERATURE REVIEW

The outcome of each NDT method depends on the technology and the testing method

type. Selecting the testing method is based on the cost and time required for the test.

Some methods are very cost effective but they are less accurate such as visual inspection

method. Historically, this method was used in a study conducted to identify the saw

marks in wood materials; the testing result was either a "Yes" for the good parts or a

"No" for the defective parts. The sliding scale was used to identify the level of defects by

choosing a range from 1 to 10, in which 1 represents the minimum, while 10 is the

maximum (Smith, Callahan, & Strong, 2005).

Newer testing technologies based on spectroscopy use ultrasonic NDT methods. The

fundamental principle of this method is based on the ultrasonic wave propagation through

the part; these waves are of such high frequency that they exceed the human hearing

ability. The wave penetrates the part at certain characteristics such as specific velocity

value; any reflection of this wave indicates a defect or flaw in the part's material (IAEA,

2001). (Characteristics such as velocity and displacement can be measured to detect the

presence of flaws in the part)

Another method called Damage Locator Vector (DLV) has been used to detect the flaws

and damage in the part's material. This method is based on vibrational testing by using

the frequency response function. The defective part is identified due to change in the

stiffness when compared to the good part (Huynh & Tran, 2004).

Another method of NDT is called the Shearography, which is used to define the invisible

defects. The principle of this technique is based on applying a laser beam on the part

under investigation. When a mechanical load is applied on the part, the defects cause a

deformation that can be detected from the reflected laser beam. This method is fast to

perform and the acquisition process and analysis takes relatively short time. The

disadvantage of this method is the incapability of testing large parts (Huke, Focke,

Falldorf, Kopylow, & Bergmann, 2010).

Figure 2.1. **Digital Shearography system** (Huke,
Focke, Falldorf, Kopylow, & Bergmann, 2010)

Resonance testing uses the vibration response of the part under excitation to detect

defects and flaws. This vibrational response of this sample when it is under excitation

contains the displacement or velocity signals for that sample. Prior to this work,

resonance testing was performed in the lab using Process Compensating Resonance

Testing (PCRT) setup which has transducers that excite the part under investigation, and

they collect the vibrational data. This process is fast to perform and more accurate than

the conventional NDT methods (Subramanian, 2013).The good and bad parts can be

recognized from the frequency output speckles. The disadvantage of this method is the

contact between the part and the transducer which makes it difficult to test complex geometry parts.

Recently, a continuous laser scanning via Laser Doppler Vibrometry (LDV) was performed on a wind turbine to analyze the vibrational characteristics. The response was measured to identify the mode shapes of the moving turbine (Yang & Allen, 2012). This method used the Vibrometer on rotating parts.

LDV is a device used for measuring vibrational characteristics of a structure under vibration loading. It has been used in recent years in aerospace (aircraft composite structure defects analysis), automotive, and biological materials such as fruits (Santulli & Jeronimidis, 2006). The results show the velocity amplitudes of fruits under excitation, if these amplitudes are in the acceptable frequency range, the fruit could be considered as good. An experiment was conducted by employing the LDV to analyze the linearity and nonlinearity of vibration characteristics to detect the defects and flaws in the deformed structures (Vanlanduit, Guillaume, Schoukens, & Parloo, 2006).

 The dynamic vibrations and Echo tests are performed in many engineering fields such as civil engineering to define the imperfection of the products and material. In these types of tests, a pulse wave is used to excite the part or the structure by a hammer, the analysis of this method is applied by observing and analyzing the reflected waves (Wong & Toppings, 1988). Using the Vibration modal analysis started in the 1970's when the FFT analyzer was developed during that time (Schwarz & Richardson, 1999). It is very important to understand and define the resonance frequencies of a part or structure because at some of these frequencies the structure can have a high amplitude response that can cause the structure damage. In a recent paper, a new testing approach using the

Laser Scanning Vibrometer was used to detect the flaws in the material (Breaban,

Carlescu, Olaro, & Gh. Prisacaru, 2011). In this experiment a PSV-300 laser Vibrometer

was used to measure the micro displacement in a velocity response form of the polymers

as illustrated in Figure 2.2. In this experiment, a white noise vibration signal was used to

identify the resonance frequencies of the part under investigation (Breaban, Carlescu,

Olaro, & Gh. Prisacaru, 2011).

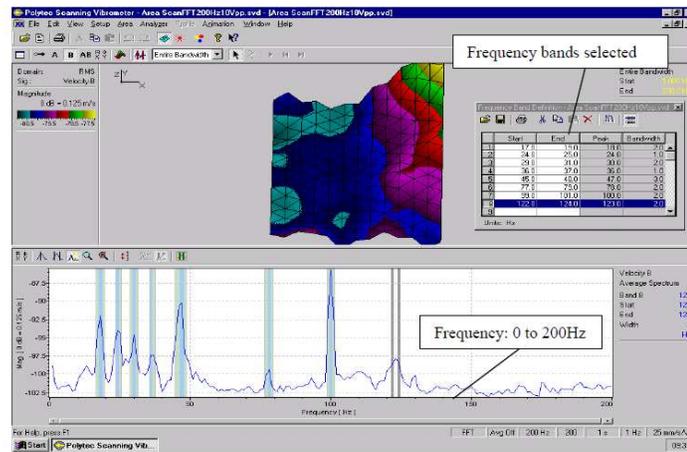*Figure 2.2.* **PSV Frequency Domain Response** (Santulli & Jeronimidis, 2006)

  Laser Vibrometer can be used for micro-scanning, by coupling the scanning head to a

microscope in order to get very small laser beam diameter (1 µm) for measuring non

periodic motions. This technology has been applied for testing gyroscopes, micro

switches, and micro motors (Traynor). The setup of this system is shown in Figure 2.3.
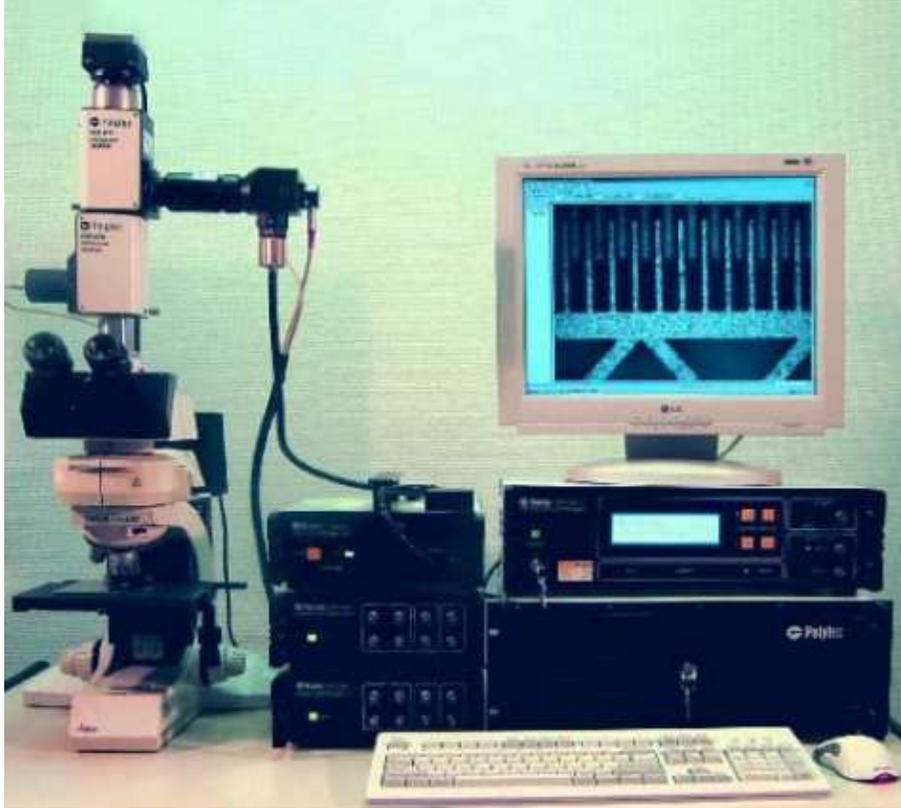
Figure 2.3. **Micro-Scanning Vibrometry** (Traynor)

Many techniques have been used to analyze the vibration testing data. In the paper by Vanlanduit et al Singular value decomposition (SVD) was proposed as a classification method, the robust SVD employed for this purpose and applied on aluminum testing data under different conditions such as fatigue, saw cut, covered with plastic, and covered with acoustic material. Most of the work was focused on a good part and defective cases, one with small fatigue crack and the other with large fatigue crack (Vanlanduit, Parloo, & Guillaume, A Robust Singular Value Decomposition to Detect Damage Under Changing Operating Conditions and Structural Uncertainties). Fig 2.3., illustrates the difference in the peaks among the good and defective parts.
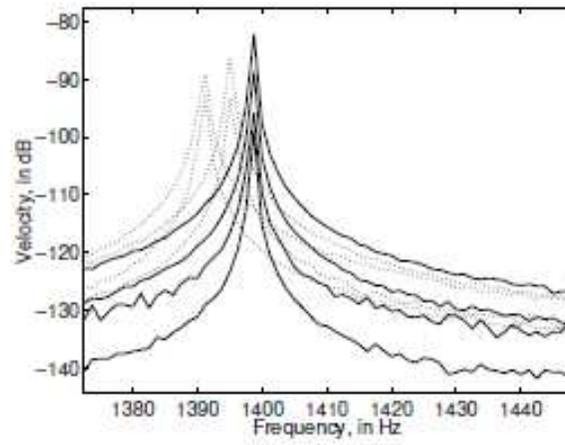
Figure 2.4. **Good (Solid lines) and Defective (Dotted lines) Parts [14]**

Chapter 3

LASER SCANNING VIBROMETER

3.1 Resonance Testing

Resonance testing is a form of NDT testing in which the part under investigation is subjected to vibrational excitation. Resonance frequencies represent a property of part or structure, the value of these frequencies depends on the material type, stiffness and boundary conditions of that structure (Schwarz & Richardson, 1999). The response of the vibration can be obtained in two forms, the time domain and frequency domain.

3.2 Vibrometer Setup

Laser Scanning Vibrometer is an instrument that uses laser beam to measure velocity of two dimensional surfaces. In this work, the main purpose of using this instrument is to measure the velocity response of a part under excitation. The generated wave in the controller can be selected in different forms such as Sinusoidal Sweep, Burst Chirp, White Noise and Square waves. The instrument is equipped with a velocity decoder that decodes the velocities in the controller unit. The range of the wave's frequencies is from 0.01 Hz to 30 MHz (Polytec). This instrument is ideal for testing parts where it is difficult to place an accelerometer like turbine blades and any other parts under vibration or movement effects.

3.2.1 Components of the Vibrometer

The instrument consists of:

1. Controller unit

2. Scanning head

3. Junction box

4. Workstation PC

Figure 3.1. **Polytec Vibrometer System**

Figure 3.2. **Laser Scanning Head**

The controller unit generates the vibration signal and decodes the velocity output signal of the part under investigation. The scanning head has interferometers to reflect the laser beam. The connection interface between the units is provided by the junction box which connects the controller to the workstation PC. The PC is provided with Polytec Scanning Vibrometer (PSV) software, this software has the ability to generate a scanning mesh points and has multiple scanning options such as continuous, single shot, and mesh scanning.

3.2.2 Fundamental principle of Laser Scanning Vibrometer

The vibrational signal is generated in the controller unit in order to excite the object to be tested, this signal could take any of these forms that are mentioned in section 3.2.

The generated laser beam passes through a beam splitter (BS1) in the scanner head, the beam splits into two beams, object and reference beams, then the object beam goes into the second splitter (BS2) and $\lambda/4$-plate which converts the linear polarized into a circular beam (Polytec). The mirrors reflect the beam to the surface of the part under investigation. A third beam splitter (BS3) splits the reflected beam from the object; one beam goes to the detector, while the other goes to the Bragg cell which determines the velocity sign (Polytec). Figure3.3. illustrates the principle of the laser beam in the Vibrometer. In order to increase the accuracy of the testing process and to ensure higher data quality, the scan and data acquisition does not start unless the signal is triggered. This triggering minimizes the time domain data errors.
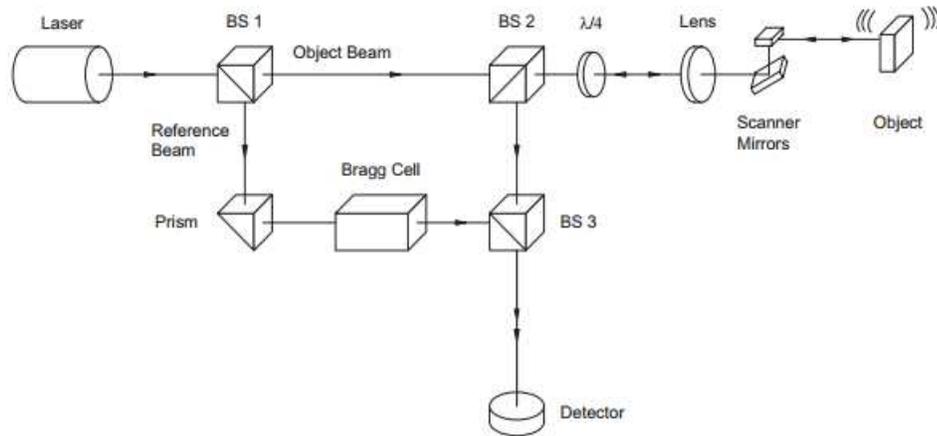
Figure 3.3. **Optical Configurations in Laser Scanner** (Polytec)

3.2.3 Advantages of using Laser Scanning Vibrometer

Laser Vibrometer provides many advantages when compared to other vibrational signal generators and acquisition systems.

1. No surface contact is required

2. A signal can be generated in the same system

3. The system uses safe helium laser

4. Can measure velocities at multiple ranges (μm/s to 30 m/s) and displacement (nm to more than 41 mm)

5. Acquire data and triggers signal at the same time.

3.2.4 Polytec Scanning Vibrometer (PSV) software

The part under investigation has to be attached to the shaker, and then the laser beam has to be pointing at the surface of the part. A mesh consists of many nodes is generated on the surface, this allows the laser beam to move at each point while sweeping the part at certain frequency range. In this project, the signal types are Burst Chirp, Sinusoidal, and White Noise with frequency range of (0-5) KHz. While sweeping the part with each signal separately, the laser beam starts the data acquisition at each point of the mesh until all points are scanned. The data in the PVS software is in two forms, time domain data (velocity vs. time) and frequency domain (velocity vs. frequency). Both data can be analyzed in the PVS to determine the mode shapes and amplitudes for the good and defective parts, the data can exported as a text file to be analyzed in MATLAB.

The PVS software has two modes, one is the acquisition, and the other is the presentation mode. The acquisition mode has a live video image of the part on which the laser beam can be moved to positions where the alignment of coordinates occur, then the mesh can be defined on the part in squares or triangular shapes. The mesh divides the part into many elements and each element has node at each corner that connects it to the neighbor element.
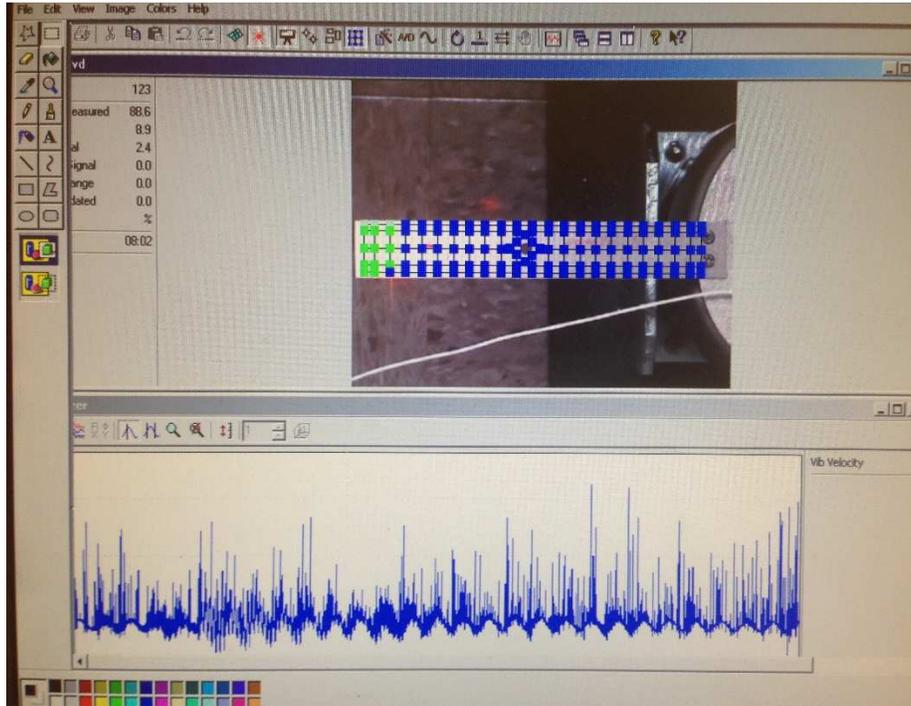
Figure 3.4. **Snapshot of Acquisition Interface**

In the acquisition mode, the setting has to be completed before running the test. Two important settings have to be set, the first is to select the frequency range, and the second is selecting the amplitude and wave type.

The output of the test is showing in small windows called analyzer. The output type can be selected as velocity or displacement in frequency or time domain, the analyzer is on X-Y coordinates. The scanning process starts with points alignment by selecting points on the objective surface, then moving the laser beam to ensure high laser concentration on the surface in case of surface flatness problems. Then, the next step before scanning process is applying the mesh on any required area of the object. Once these settings are completed, the acquisition process can start by sweeping all the nodes of the mesh.

16
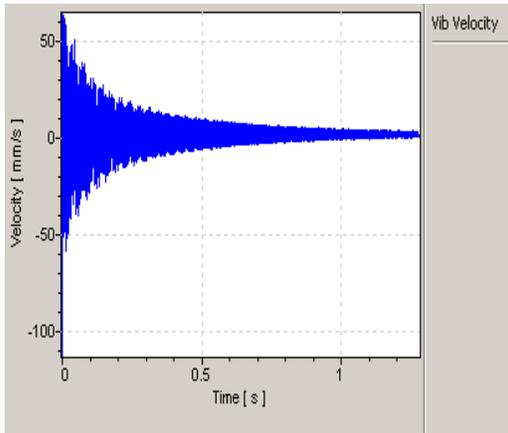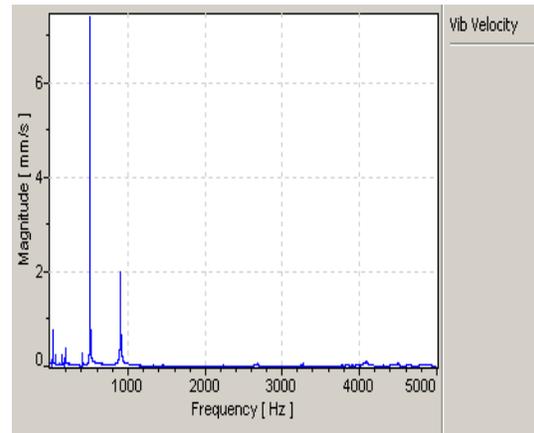
a- Time Domain   **b- Frequency Domain**

Figure 3.5. **Time and Frequency Domain Response**

The second mode of the PVS software is the display mode in which the analysis on the data can be performed such as selecting the highest amplitudes, define the mode shapes, and calculating the magnitude and phase of the velocity and displacement signals. The output can be displayed in 2D, 3D, animation, or single points. Any of these display methods can be applied on the velocity or displacement output.
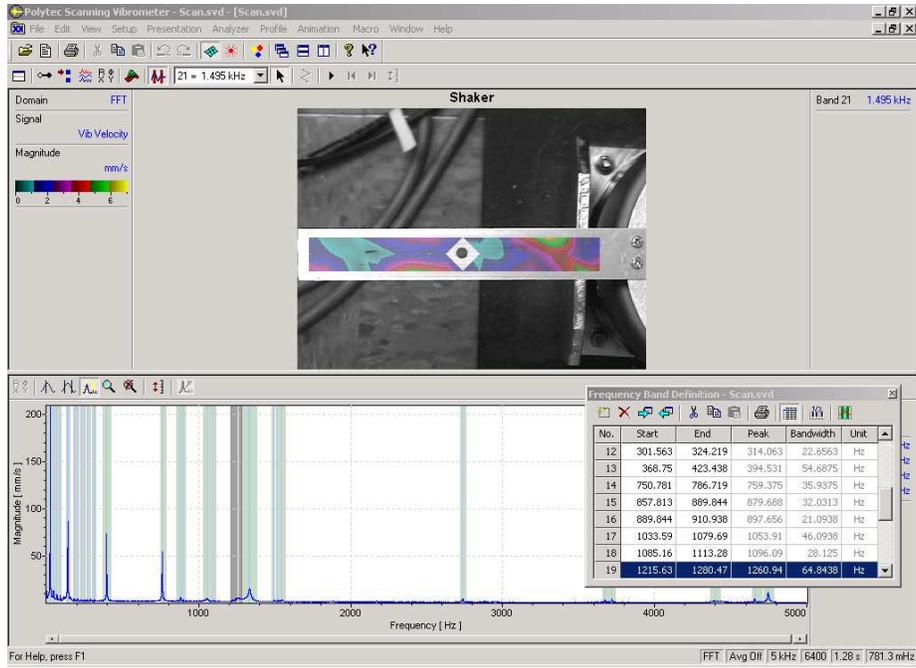
17

Figure 3.6. PSV Display Mode
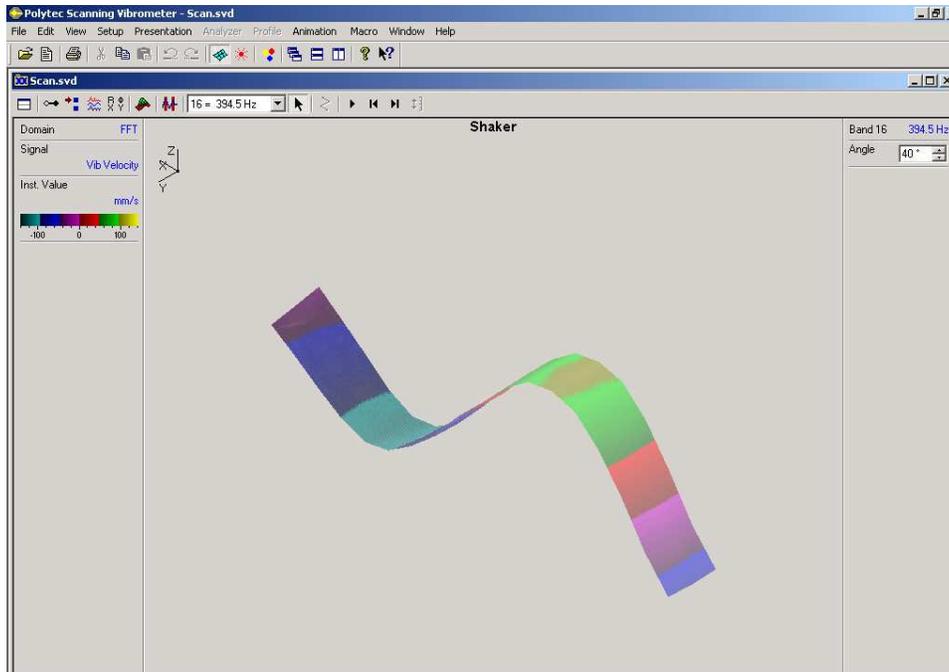
Figure 3.7. 3D Mode Shape Display

18

3.3 Experimental Samples

The samples are made of aluminum-6061 T6 which has the properties listed in Table 3.1.

Table 3.1
Aluminum properties in SI units

Property	Value
Density	2700 Kg/m^3
Modulus of Elasticity	68 Gpa
Poisson's Ratio	0.33

The dimensions of the samples are 201.68 mm X29.337 mm X 1 mm. The defective

parts have a hole of 6.35 mm diameter, the center of the hole is located at distance 93.726

mm from the free end of the sample.

Figure 3.8. **Defective Sample**

While performing the experiments, each sample must be attached permanently from one

side to the top surface of the shaker using two bolts.

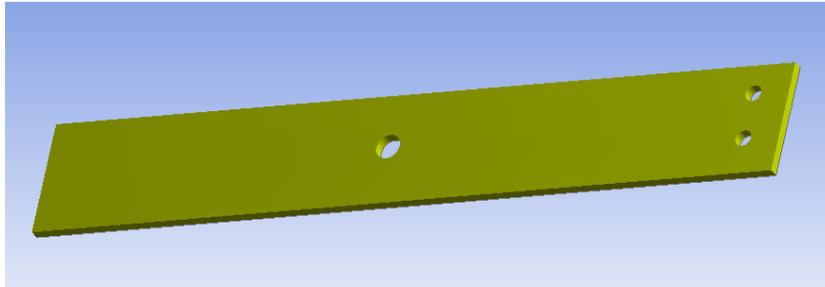A Labworks shaker model (ET-139) is employed for this work. This shaker has vibration frequency range of up to 6.5 KHz and it can be used for general vibration testing.

Chapter 4

ANALYSIS METHODS

The analysis is performed on a cantilever beam on the defective and non-defective parts.

This type of beam has one of its ends fixed and the other end is free as illustrated in

Figure 4.1.
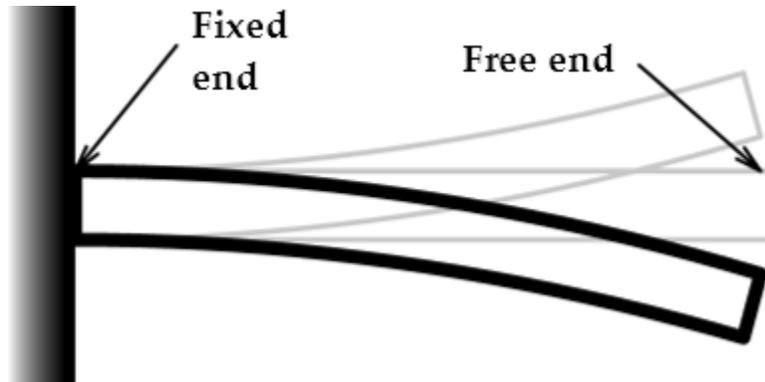
Figure 4.1. **Cantilever Beam**

4.1 Modal Analysis Using Finite Element Analysis (FEA)

A simulation of both good and bad parts was created in ANSYS and NASTRAN NX8.0

to analyze the modal and harmonic characteristics such as mode shapes and resonance

frequencies of the part as shown in Figure 4.2. This simulation represents the ideal

conditions of the vibrational test. The resonance frequencies can be compared by

observing the location of the peaks, in which the defective part shows a skewing of the

peaks to the right. Another way to compare the resonance frequencies is by observing the

ANSYS modeling frequency output table, which shows the difference between both

parts.
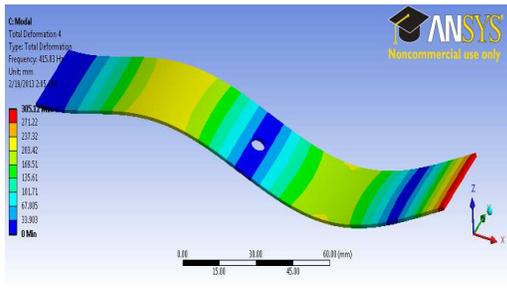
A- Defective
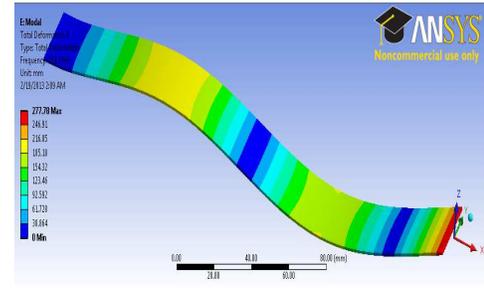
B- None-defective

Figure 4.2. **ANSYS Simulation of Defective and Non-Defective parts**

The modes and natural frequencies of any system can be obtained by mathematical

equations in analytical or numerical methods. The analytical method requires

representation of the system in mass-spring form by generating the equation of motion

$$[M]\{\ddot{X}\}+[C]\{\dot{X}\}+[K]\{X\}=0 \qquad (4.1)$$

In which

[M] is the mass of system

[C] is the damping constant

[K]is the stiffness

$\ddot{X},\dot{X},X$ are acceleration, velocity and displacement respectively.

The natural frequency of the system is found by the equation:

$$\omega_n = \sqrt{\frac{k}{m}} \qquad (4.2)$$

The mode shapes and corresponding frequencies depend on the boundary conditions. In this work, the samples are fixed from one side and free on the other side (cantilever beam). The equation of motion of a cantilever beam:

$$\frac{d^2}{dx^2}[EI\frac{dY(x)^2}{dx^2}]=\omega_n m(x)Y(x) \tag{4.3}$$

Where:

E is the modulus of elasticity

I is the moment of inertia

Y(x) is the displacement in Y-direction

ω_n is the natural frequency

Boundary conditions of a cantilever beam are:

$Y=0$ at x=0, no deflection at the fixed end

$\frac{dY}{dx}=0$ at x=0, no angular deflection at the fixed end

$\frac{d^2Y}{dx^2}=0$ at x=0 and x=L, no bending moment at the free end

$\frac{d3Y}{dx^3}=0$ at x=L, no shear force at the free end

By applying the boundary conditions on the equation of motion of the cantilever beam, the frequency equation can be obtained:

$$\cos\beta_n L+\cosh\beta_n L=-1 \tag{4.4}$$

Where $\beta^4=\frac{\omega_n^2 m}{EI}$

Now the mode shapes equation can be obtained for a cantilever beam:

$$f(x) = A[(\sin \beta L - \sinh \beta L)(\sin \beta x - \sinh \beta x) + (\cos \beta L + \cosh \beta L)(\cos \beta x - \cosh \beta x)]$$

(4.5)

Mode shapes and corresponding frequencies values depend on the material properties and boundary conditions. For a cantilever beam these values are listed in Table 3.2.

Table 4.1
Natural frequencies of first three modes

Mode	Natural frequency
First	$\omega_n = 3.515\sqrt{\dfrac{EI}{\rho AL^4}}$
Second	$\omega_n = 22.03\sqrt{\dfrac{EI}{\rho AL^4}}$
Third	$\omega_n = 61.7\sqrt{\dfrac{EI}{\rho AL^4}}$

4.2 Mathematical Model

The model of each dynamical system represents the behavior and characteristics when a specific input signal is applied, then depending on these characteristics, the system responses with an output signal. In this work, many models in different forms are predicted and evaluated using the experimental data. The time domain data of a non-defective part is selected to perform this analysis. The predicted system models are used to calculate the output $y(t)$ when a specific input signal $u(t)$ is applied. Input signal is a sine sweep of 0.01-5000 KHZ, half of the signal data is used to generate the model and the other half is

used for validation. The predicted models quality can be measured by a parameter called

Final Prediction Error (FPE), which is given by:

$$FPE = V(1 + \frac{2d}{N}) \qquad (4.6)$$

Where:

V is the loss function

d is number of estimated parameters

N is number of values of the data set

This parameter is used to compare the predicted models. The quality of models increases

when the FPE value is reduced.

The types of evaluated models are:

a. Autoregressive-moving average model with exogenous component (ARMAX)

It is a time series model used for simulating and predicting economics and industrial

behavior. This model was introduced by Wold (1938) as a combination of

Autoregressive and Moving average models (Makridakis & Hibon). The model

equation consists of multiple polynomials and it can be written as

$$Ay = Bu + Ce \qquad (4.7)$$

In MATLAB, the order of each polynomial is described and has a value which can be

adjusted to get the best model results.

n_a Order of the polynomial A(q)

n_b Order of polynomial B(q)+1

n_c Order of polynomial C(q)

n_k Input-output delay

This model has been used to represent the relationship between the input and output of a system (Fung, Wong, Ho, & Mignolet, 2003). The experimental time series data (Time –Velocity) can be imported to MATLAB workspace, then a selection of ARMAX model parameters can be done by iterations until the best model fit is reached.

b. Box-Jenkins model (BJ)

It is a method uses time domain data to predict a system model. The method follows five steps to select, identify and perform an assessment on conditional mean models (Mathworks, n.d.). The steps of predicting the model are:

1. Keeping the time domain series stationary

2. Predicting the stationary for the data

3. Estimating the model parameters

4. Performing goodness fit checks to ensure the system is describing the experimental data

5. Generating Monte Carlo simulations for the future time data

The equation of the model is

$$y = \frac{B}{F}u + \frac{C}{D}e \qquad (4.8)$$

During performing the model analysis in MATLAB, the order of each polynomial must be estimated in order to get the best fit. The notation of each polynomial order are:

n_b Order of B polynomial+1

n_c Order of C polynomial+1

n_d Order of D polynomial+1

n_f Order of F polynomial+1

n_k Input delay

c. Output-error model (OE)

   This model is generated when the disturbance is affecting the output signal (Jamil,

   Sharkh, & Hussain, 2008). The output is represented as a function of the input and the

   error.

d. System transfer function (TF)

   The transfer function approach is used for modeling and analyzing dynamical systems.

   This approach characterizes the input-output relationship of a dynamical system in a

   form of mathematical equation that expresses the differential equation which relates

   input signals to output (Ogata, 2004).

   Once the transfer function of a system is known, then the response of that system

   can be determined for any input signal. Each transfer function can be represented as a

   block diagram as shown below.

$$x(s) \rightarrow \boxed{G(s)} \rightarrow y(s)$$

 Where

$G(s) = \dfrac{y(s)}{x(s)}$ is the transfer function of a system.

4.3 PSV Analysis:

The frequency domain data can be simulated in the PSV software to get the mode shapes and amplitude peaks for both good and bad parts.

The response from the laser Vibrometer is in two forms, time domain and frequency domain. In the time domain, the collected velocity data is varying during (1.27 seconds) time period. While in frequency domain, the velocity is varying depending on the value of the frequency. As it illustrated in Figure 3.5., the velocity response has some amplitudes at certain frequencies. These amplitudes are generated at the resonance frequency of the part.

4.4 Discriminant Analysis

It is a method used for classification when there is more than one group that differ in some parameters' values or types. This method is used to distinguish between these groups. A fitting function is employed to create the class type from experimental training data which is used to classify any data under investigation to recognize which group it is belong to.

4.4.1 Purpose of discriminant analysis:

1. Creates a model that describes the difference between patterns with different classes in terms of parameters

2. Predicts the class of unclassified testing data

4.4.2 Fisher Discriminant Analysis

It is a technique that produces a discriminant function to classify two types of data by creating a projection on a line in such a way that samples are separated into their classes (Bishop, 1995). This technique increases the difference of variance between the classes with respect to the variance of data of each class. If n_1, n_2 are two samples for class1 and

28

class2 respectively then the projection y_i of element x_i in the w direction can be given by the scalar dot product:

$$y = w^t x \tag{4.9}$$

In Fisher's discriminant analysis both sample classes are projected on the line, the difference between the means of the projected samples is used as a classification measure. The mean of sample 1 and 2 are:

$$\mu_1 = \frac{\sum_{x \in D_1} X}{n_1} \tag{4.10}$$

$$\mu_2 = \frac{\sum_{x \in D_2} X}{n_2} \tag{4.11}$$

Where D_1 and D_2 are data of group1 and 2 respectively.

Then the means of the projected samples are given by

$$\widetilde{\mu_1} = \frac{\sum_{x \in D_1} w^t x}{n_1} = w^t \mu_1 \tag{4.12}$$

$$\widetilde{\mu_2} = \frac{\sum_{x \in D_2} w^t x}{n_2} = w^t \mu_2 \tag{4.13}$$

Also the difference between the means is given by

$$\widetilde{\mu_1} - \widetilde{\mu_2} = w^t (\mu_1 - \mu_1) \tag{4.14}$$

The scatter of the projected samples is

$$\widetilde{s_1}^2 = \sum_{y \in P_1} (y - \widetilde{\mu_1})^2 = \sum_{x \in D_1} (w^t x - w^t \mu_1)^2 = \sum_{x \in D_1} w^t (x - \mu_1)(x - \mu_1)^t w \tag{4.15}$$

$$\tilde{s}_2^2 = \sum_{y \in P_2} (y - \widetilde{\mu_2})^2 = \sum_{x \in D_2} (w^t x - w^t \mu_2)^2 = \sum_{x \in D_2} w^t (x - \mu_2)(x - \mu_2)^t w \qquad (4.16)$$

Where P_1 and P_2 are the projected data of both class samples.

In this discriminant analysis, the linear relationship between the original and the projected data maximize the following criterion:

$$J(w) = \frac{(\widetilde{\mu_1} - \widetilde{\mu_2})^2}{\tilde{s}_1^2 + \tilde{s}_2^2} \qquad (4.17)$$

Since this classification based on the direction of the projection line, thus it is necessary to evaluate the criterion $J(w)$ as an explicit function of w. The scatter matrices are calculated in terms of the mean and the data of each sample and they can be written as:

$$S_1 = \sum_{x \in D_1} (x - \mu_1)(x - \mu_1)^t \qquad (4.18)$$

$$S_2 = \sum_{x \in D_2} (x - \mu_2)(x - \mu_2)^t \qquad (4.19)$$

The summation of both scatter matrices is given by

$$S_w = S_1 + S_2 \qquad (4.20)$$

Then equations (4.15) and (4.16) can be written as

$$\tilde{s}_1^2 = w^t S_1 w \qquad (4.21)$$

$$\tilde{s}_2^2 = w^t S_2 w \qquad (4.22)$$

Then

$$\tilde{s}_1^2 + \tilde{s}_2^2 = w^t S_1 w + w^t S_2 w = w^t (S_1 + S_2) w \qquad (4.23)$$

Substituting equation (4.20) leads to

$$\tilde{s}_1^2 + \tilde{s}_2^2 = w^t S_w w \qquad (4.24)$$

30

Similarly the numerator of equation (4.17) can be obtained in terms of w

$$(\widetilde{\mu_1} - \widetilde{\mu_2})^2 = (w^t \mu_1 - w^t \mu_2)^2 \qquad (4.25)$$

$$= w^t (\mu_1 - \mu_2)(\mu_1 - \mu_2) w \qquad (4.26)$$

Then simply $J(w)$ can be found as a function of w

$$J(w) = \frac{w^t S_B w}{w^t S_w w} \qquad (4.27)$$

Where $S_B = (\mu_1 - \mu_2)(\mu_1 - \mu_2)^t$

  For better classification results, the greater the difference between the projected samples means the better the classification.

$$J(v) = \frac{(\mu_{p1} - \mu_{p2})^2}{s_{p1}^2 + s_{p2}^2} \qquad (4.28)$$

The greater the difference between the projected means leads to more accurate classification.

4.6 Neural Network

This classification method uses the input training data to generate an output classification pattern. This method can be used to solve different types of problems by using some tools such as fitting, pattern recognition, clustering, and time series tools. In this work, a neural network is used to classify train the experimental data sets into two classes, then according to the output classification, the classifier used to test any other sets of data. The network consists of two layers, one is hidden and the second is the output neurons, the range of the output signal is 0-1. In this analysis, a frequency-velocity data is imported in MATLAB. This data contains data of ten non-defective and ten defective samples. Each sample has

6400 sampling rate, so the total of samples is 128,000 of either 0 or 1 output. The type of the network is two-layer feed-forward with sigmoid hidden and output neurons, which means that the input data information is moving in only one direction (forward) and it does not have any loops. The network uses a back propagation in order to update the values of bias and weights by estimating the gradient through the conjugant gradient method. The fundamental principle of Neural Network is based on the values of the classified data, and depending on the weight of the values, the class type is identified. The Network consists of nodes connected by arrows, each arrow has a specific direction and weight. The main process occurs in the hidden layer which decides the type of the class based on the weight value as illustrated in Fig [4.4], the green arrows represent the greater value of weight while the blue arrows represent the smaller values; then according to that, node "C" chooses the value from input node "A", and node "D" selects the input "B". The hidden layers send the class information to the output to compare it with the desired values (0, 1). The network error can be determined by subtracting the hidden layers output from the desired output. The back propagation technique in the network is used to reduce the error value until the lowest value of error is reached. This technique is an effective computational method for finding the error function with respect to the network weights (Bishop, 1995).
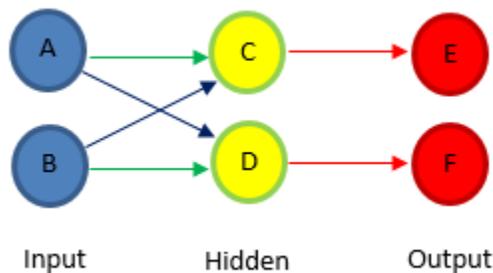

Figure 4.3. **Neural Network Layers**

The network input and hidden layers contain bias values. The network in Fig 4.5.,

consists of input layer(x), hidden layer (z), and output layer (y). The weight can be

calculated by combining the bias of the jth hidden element (w_{j0}^1) with the weight of the

input layer (w_{ij}^1) (Bishop, 1995), and it can be written as:

$$a_j = \sum_{i=1}^{d} w_{ji}^1 x_i + w_{j0}^1 \tag{4.29}$$

For simplicity, the bias term could be eliminated and equation (4.29) could be rewritten

as:

$$a_j = \sum_{i=1}^{d} w_{ji}^1 x_i \tag{4.30}$$

A continuous sigmoidal function is used to activate the hidden unit (z_j) which is

represented in equation (4.31)

$$z_j = g(a_j) \tag{4.31}$$

Since this network contains two layers, the second layer is used to compute the

output. Then the output of the hidden units can be represented in the same way used in

the first layer

$$a_k = \sum_{i=1}^{m} w_{kj}^{(2)} z_j \tag{4.32}$$

In order to obtain the activation of the kth output, the linear equation (4.32) could be

transformed using a nonlinear function $\tilde{g}(.)$ (Bishop, 1995).

$$y_k = \tilde{g}(a_k) \tag{4.33}$$

The final network equation is written in the following form

$$y_k = \tilde{g}(\sum_{j=0}^{m} w_{kj}^{(2)} g(\sum_{i=0}^{d} w_{ji}^{(1)} x_i))$$
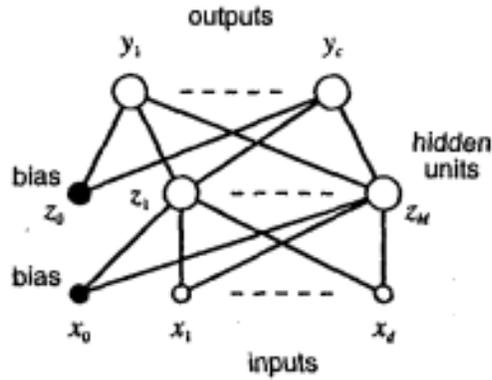
(4.34)

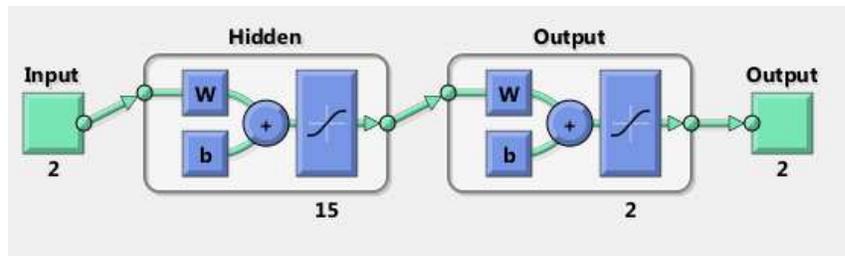*Figure 4.4.* **Feed-Forward Network with Two Layers** (Bishop, 1995)

Figure 4.5. **Neural Network Design in MATLAB**

The percentage of well and misclassified data for training, testing, and validation is estimated by a confusion matrix. The diagonal shows correct predictions, while the other values show the incorrect prediction or the misclassified data.

Figure 4.6. **Confusion Matrix**

The neural network toolbox in MATLAB splits the data into three groups training, validation, and testing. The percentage of each group is selected by user and can be adjusted to get better classification results. The training and validation groups affect the training process by adjusting the error and the generalization of the network until the generalization stops improving.

4.6 Hilbert Huang Transform

Hilbert Huang Transform (HHT) is an algorithm uses non-linear non-stationary time domain signal such as white noise wave to obtain the frequency output. This algorithm decomposes the signal into intrinsic mode functions (IMF) which are a simple oscillatory harmonic functions having the same number of highest amplitudes (extrema) and zero

crossing and it can be described on x-y graph by variable amplitudes on the y-axis and frequency along the x-axis. There are two steps to follow in order to use HHT algorithm:

1. Empirical mode decomposition (EMD)

2. Hilbert spectral analysis

  The EMD is used to convert the non- linear time domain data into IMF. A process called sifting is applied to find the IMF from given data. During this process, the local upper amplitudes and lower amplitudes of the time data are evaluated, then these amplitudes are connected by a spline line to create the upper and lower envelopes. The average of these envelopes represent the frequency component which is then subtracted from the original signal (Kim & Oh, 2009).
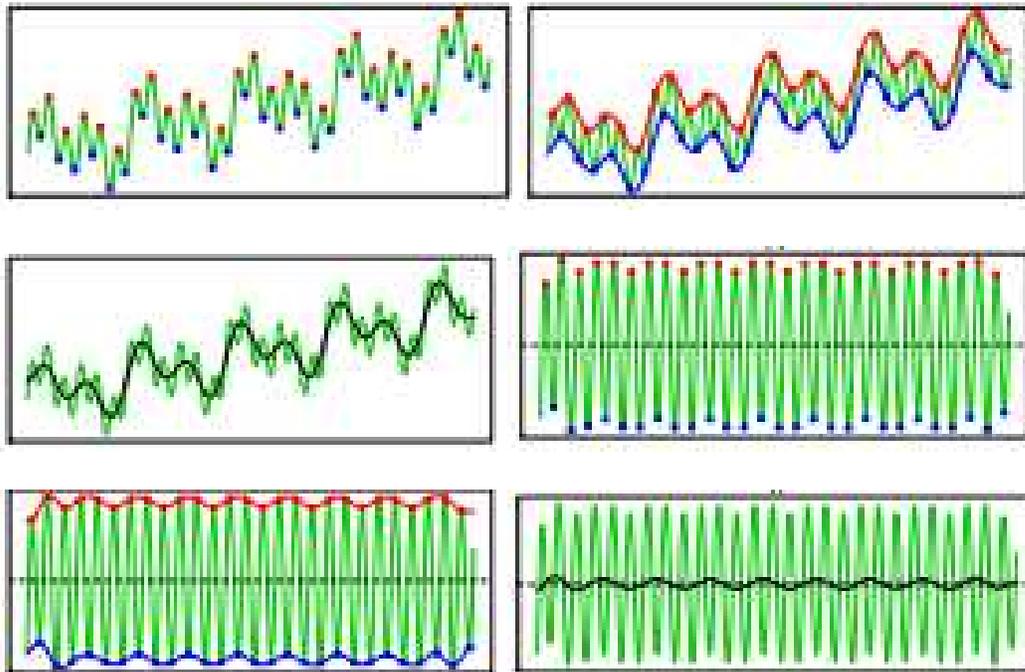

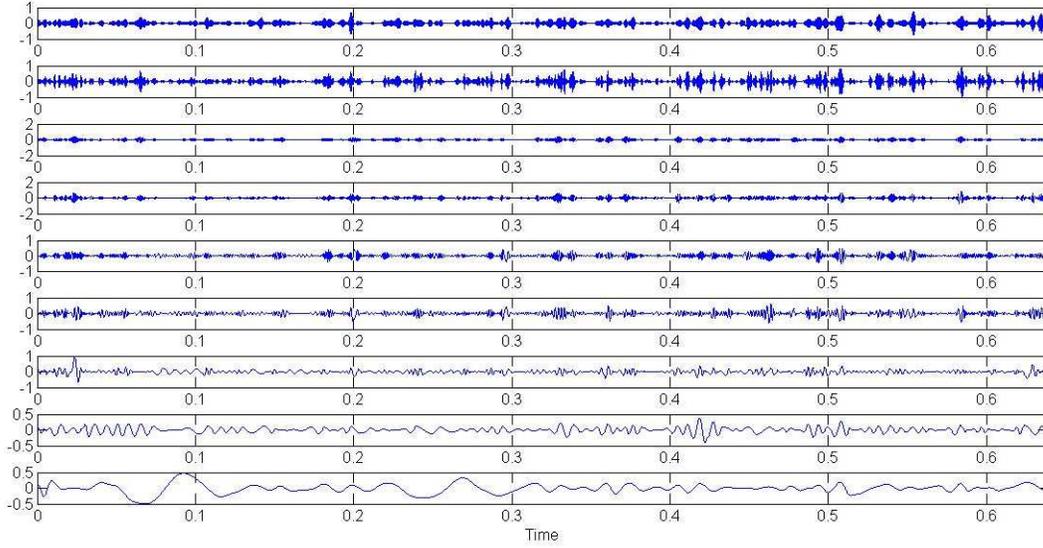*Figure 4.7.* **Sifting Process** (Kim & Oh, 2009)

Figure 4.8. **EMD Analysis for 9 IMFs**

The Hilbert spectral analysis used for evaluating the instantaneous frequency of IMF. When the time domain signal $x(t)$ which includes a velocity changes over time is non-stationary, then the evaluated analytic signal $z(t)$ is given by

$$z(t) = x(\text{t}) + \text{i } y(\text{t}) \tag{4.35}$$

Where $y(t)$ represents HHT of $x(t)$ and it is given by

$$y(t) = \frac{1}{\pi} p \int_{-\infty}^{\infty} \frac{x(s)}{t - s} ds \tag{4.36}$$

p is the Cauchy principle value. The polar equation of the analytic signal $z(t)$ is

$$z(t) = a(t) \exp(i\theta(t)) \tag{4.37}$$

Here, $a(t)$ is the amplitude or called the envelope function (Hui & Zhang, 2009) and can be written as $\sqrt{x(t)^2 + y(t)^2}$, and $\theta(t)$ is the phase which is given by $\arctan(\frac{y(t)}{x(t)})$. The

37

instantaneous frequency w is the time derivative of the phase, it is written as $\dfrac{d\theta(t)}{dt}$ and

it is showing in Figure 4.10., as amplitudes and instantaneous frequency. The Hilbert

Huang Spectrum can be expressed as a function of time and frequency

$$H(t,w) = r\sum_{i=1}^{n} a_i(t)\exp(w_i(t)dt) \qquad (4.38)$$

In equation (4.38), r is the residue (Hui & Zhang, 2009). The Local Marginal Spectrum

of the IMF function is given by

$$h_i = \int_0^T H_i(t,w)dt \qquad (4.39)$$

Once the decomposition process is applied, the decomposed Time-Velocity signal of

each Empirical mode will have an envelope function and phase. The summation of the

Empirical modes leads to the original signal $x(t)$.

$$x(t) = \sum_1^n E_i(t) \qquad (4.40)$$

Where

$E_i(t)$ The Empirical mode function
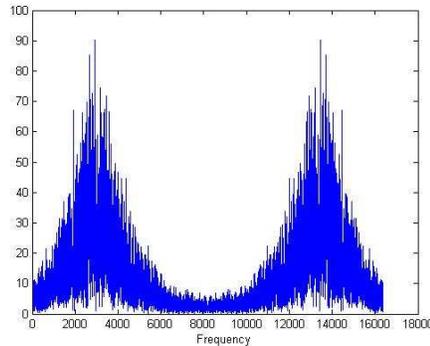
n Total number of Empirical modes

Figure 4.9. **Hilbert Spectrum**

38

Chapter 5

RESULTS

In this chapter, the techniques presented in chapter four are used for classification on the same dataset. The data was obtained via PSV Laser Vibrometer setup discussed in chapter three.

5.1 System Model

The model of the system can be identified and simulated in MATLAB by using the (velocity-time) data, and according to the relationship between the input and the output, the parameters of each model can be estimated to get the best model fit. In MATLAB there are many suggested models can be performed on any set of data using the system identification toolbox, and the final results of the simulation can be plotted over the experimental graph in order to observe the accuracy of each system. The main purpose of estimating the model for the none-defective parts is to generate an ideal model that represents the good parts, then from any collected data from other samples can be used to compare response with the ideal case. In this section, the ideal model was predicted and generated using the non-defective sample. The experimental data was collected under vibrational conditions of a sinusoidal sweep of (0.1-5) KHZ and the response was collected using the Laser Scanning Vibrometer.

5.1.1   Autoregressive-moving average model (ARMAX)

The predicted model here is a combination of Autoregressive and Moving average models with exogenous component. The parameters where found using trial and error

method in order to get the best fit compared to experimental data graph. Equation (4.7) represents ARMAX model and can be written as a function of time

$$A(q)y(t) = B(q)u(t) + C(q)e(t) \qquad (5.1)$$

$$A(q) = 1 - 3.42q^{-1} + 4.784q^{-2} - 3.307q^{-3} + 0.9436q^{-4}$$

$$B(q) = 2404q^{-1} + 4808q^{-2} - 2404q^{-3}$$

$$C(q) = 1 - 2.472q^{-1} + 2.483q^{-2} - 0.9719q^{-3} - 0.1973q^{-4} + 0.3028q^{-5} - 0.1448q^{-6}$$

Loss function: 0.0111811

FPE: 0.0112166

Sampling interval: 7.8125e-005

The block diagram of the ARMAX system is shown in Figure 5.1., where the input and output relationship can be observed including the effects of dynamical disturbance.
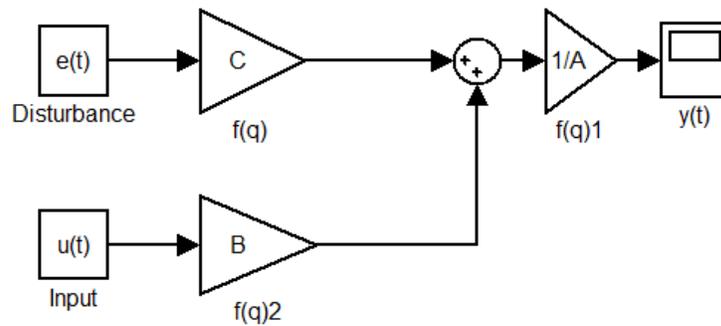

Figure 5.1. **ARMAX Block Diagram**

The order of the model polynomials are found to be

$n_a = 4$

$n_b = 3$

$n_c = 6$

$n_k = 1$

Figure 5.2. **ARMAX Parameters Setting**

The ARMAX system model is shown in Figure 5.3., plotted on top of the experimental data graph. From the output figure, it can be concluded that the model has a good fit and it represents the true model as a combination of autoregressive-moving averages models.
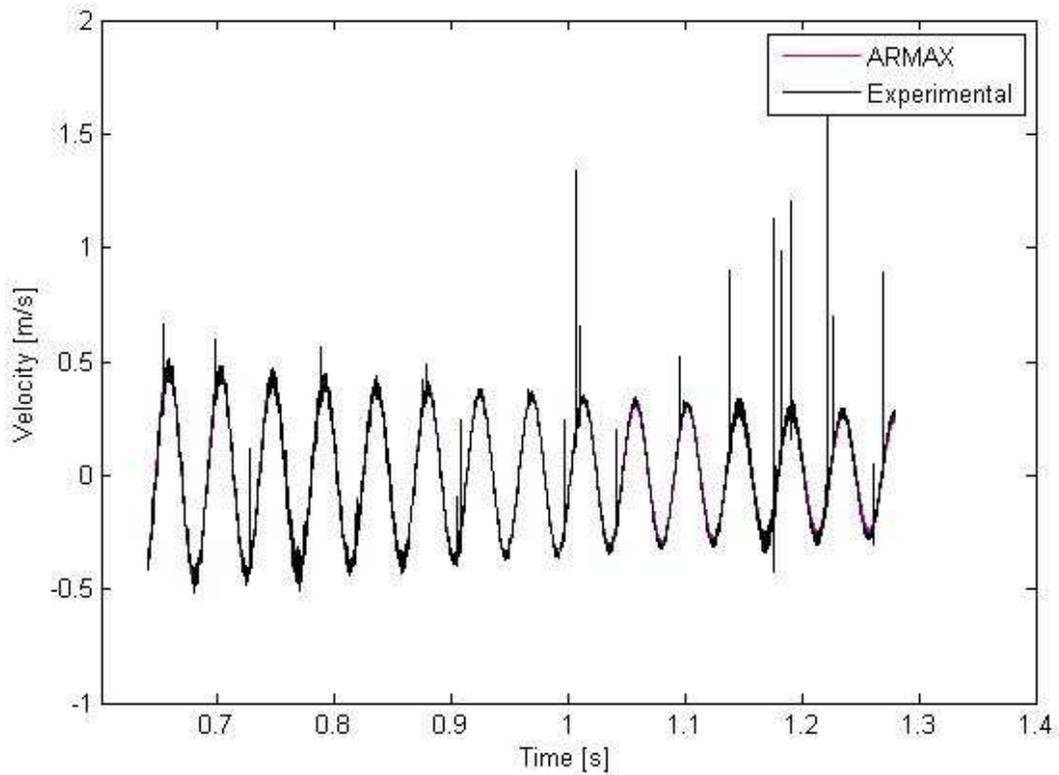
Figure 5.3. **ARMAX Model**

5.1.2 Box-Jenkins model

The general form of this of this model can be written as a mathematical equation that relates the output to the input signals that changes with time. Equation (5.2) shows the model input-output relationship:

$$y(t) = \frac{B(q)}{F(q)} u(t) + \frac{C(q)}{D(q)} e(t) \tag{5.2}$$

$B(q) = -6786q^{-4} - 2002q^{-5} + 2.436e004q^{-6} - 1.557e004q^{-7}$

$C(q) = 1 - 1.396q^{-1} + 0.08773q^{-2} + 1.225q^{-3} 0.8028q^{-4}$

$$D(q) = 1 - 2.149q^{-1} + 1.102q^{-2} + 1.192q^{-3} - 1.582q^{-4} + 0.3746q^{-5} + 0.1255q^{-6}$$

$$F(q) = 1 - 2q^{-1} + q^{-2}$$

Loss function: 0.00854264

FPE: 0.00857601

Sampling interval: 7.8125e-005

The order and the polynomial parameters are found using trial and error method. This type of model can be represented in a block diagram that relates the output to the input signal, taking in consideration the effects of the dynamical disturbance.
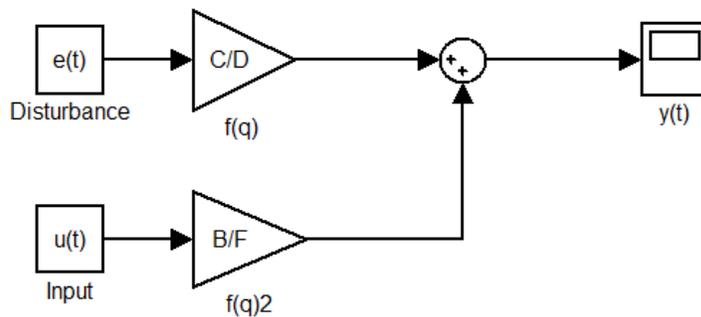

Figure 5.4. **Box-Jenkins Block Diagram**

In this model, the order of the polynomials was also estimated to get the best fit when plotted on the same graph of the experimental data.

Figure 5.5. **Box-Jenkins Parameters Setting**

The model output shows a good response and an accurate fit to the original experimental

data.
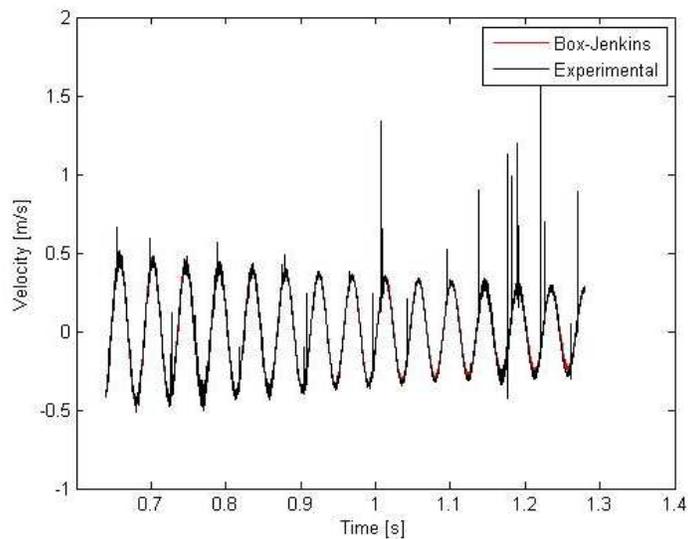
Figure 5.6. **Box-Jenkins Model**

44

5.1.3 Output-error model (OE)

The general form of the OE model can be written as

$$y(t) = \frac{B(q)}{F(q)} u(t) + e(t) \tag{5.3}$$

The values of the parameters polynomials are:

$B(q) = 2074q^{-1} - 1785q^{-2} - 2652q^{-3} + 2363q^{-4}$

$F(q) = 1 - 2q^{-1} + q^{-2}$

Loss function: 0.0230658

FPE: 0.0230996

Sampling interval: 7.8125e-005
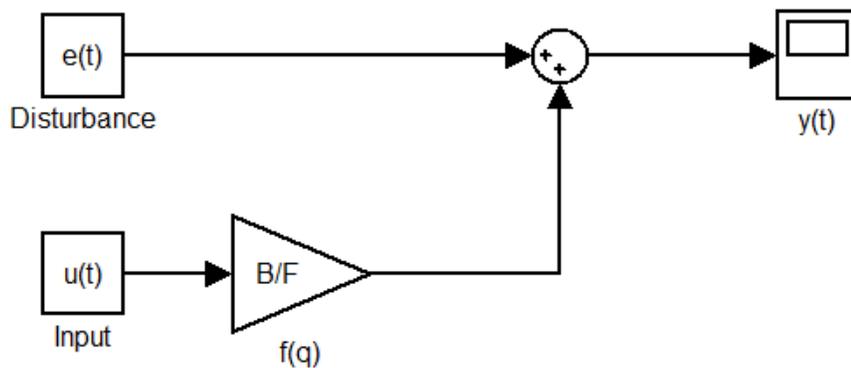
***Figure 5.7.* Output-Error Block Diagram**

The results of this model shows that the FPE is 0.0230996, which is higher than the other models; this makes OE model less accuracy.

The parameters were computed in MATLAB, also the order of the polynomials were

estimated using trial and error.

Figure 5.9 shows the estimated parameters which are selected by trial and error until best

fit is reached. The output of the model is plotted over the experimental data, as it can be

seen that the model has a good fit in approximating the system model.

Figure 5.8. **Output-Error Parameters Setting**
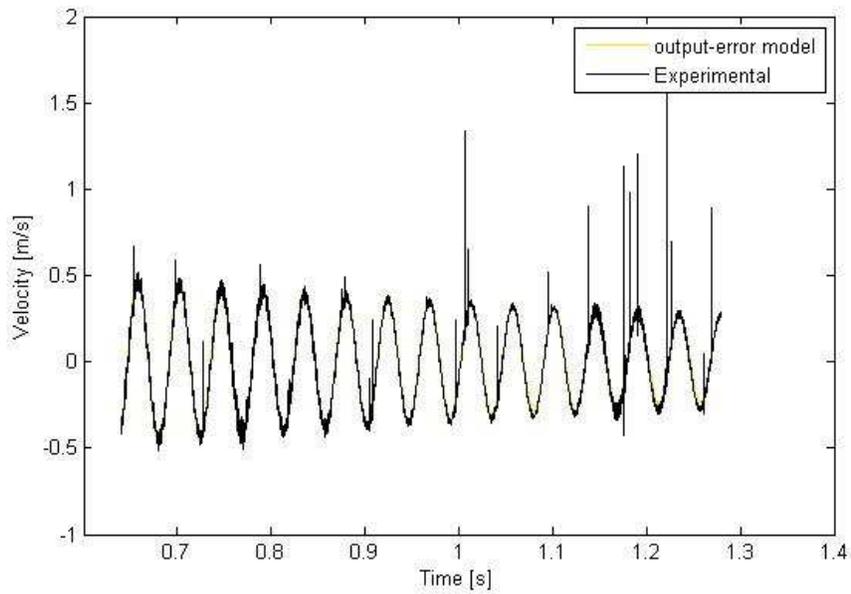
Figure 5.9. **Output-Error Model**

5.1.4   Process model transfer function

This model represents the ratio of the output to the input. The equation below is

transfer function of the cantilever beam that is used from the good sample.

$$G(s) = K_p \frac{1 + T_z s}{(1 + 2\zeta T_w s + (T_w s)^2)(1 + T_{p3} s)}$$

With

$K_p = -5$

$T_w = 0.007$

$\zeta = 0.001$

$T_{p3} = 50$

$T_z = 0.2$

A proportional gain (K_p)used which is a ratio of the controller output to the error signal

the assigned value by trial and error is -5 which gives the actual behavior of the

47

relationship between the time and velocity; moreover, increasing the time reduces the

velocity amplitudes. The damping ratio is <1 which makes the system under damped,

which also represents the real case of a cantilever beam vibration.

The model has 1 zero and 3 poles and an integrator. The zero time constant (T_z), the time

constant of the complex poles (T_W), and the time constant of real poles (T_{p3}) were

estimated to get the best accurate results.
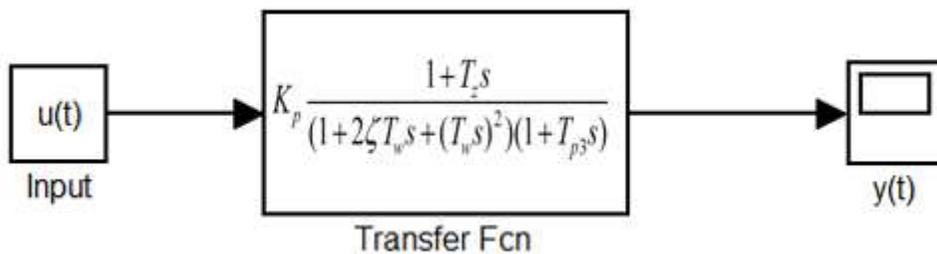
Figure 5.10. **Open-Loop Transfer Function**
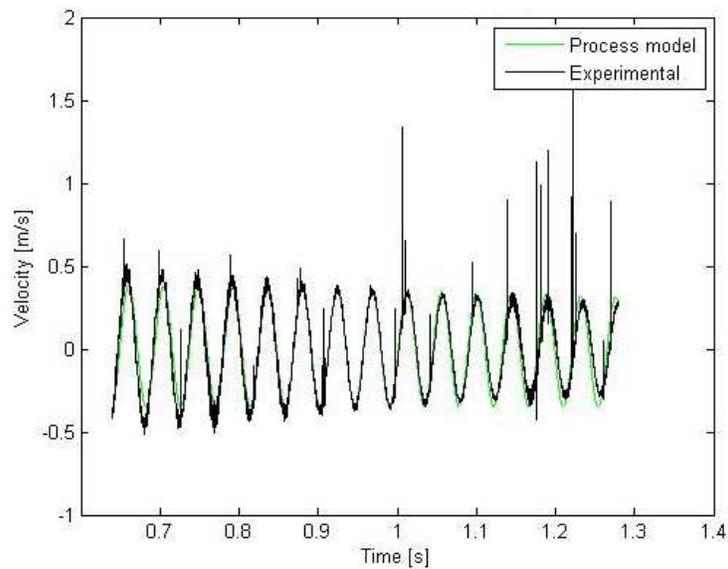
Figure 5.11. **Process Model**

48

5.2   Fisher Discriminant Analysis

This analysis was performed using 10 non-defective samples and 10 defective samples at 6400 sampling rate which leads to using 128,000 values of frequency-velocity data. In the final results, the output graph contains a curve that shows the class of any unknown data of a sample under same vibrational conditions.
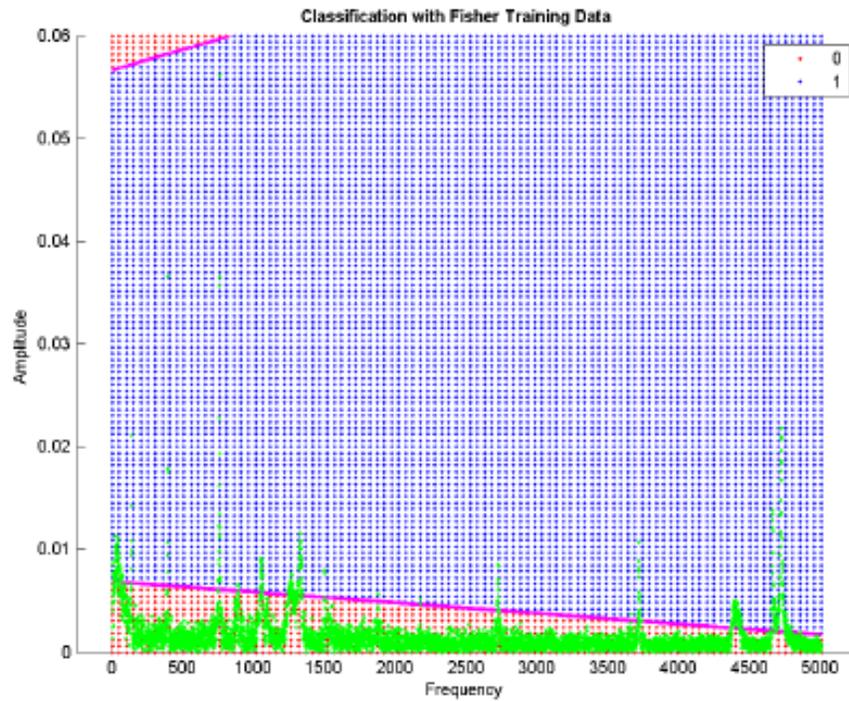
Figure 5.12. **Fisher Non-Defective Sample**

The graph of Figure 5.13., represents the non-defective part, where most of the amplitudes are below the classification curve.

49

Figure 5.13. **Fisher Defective Sample**

The defective part graph shows higher amplitudes that passes the classification line as well as some of the amplitudes reaches the the top left corner of the graph.

5.3   Neural Network Classification

The Neural network classification is performed in order to get the class output of any imported unknown sample. Once the classification is done, validation takes action to assure that the classification is accurate then a small percentage from the classification data is used for testing the classifier. The accuracy of all these classifier building stages is shown in the confusion matrix, as illustrated in Figure 5.15.

Training Confusion Matrix

	1	2	
1	32152 35.9%	7020 7.8%	82.1% 17.9%
2	12458 13.9%	37970 42.4%	75.3% 24.7%
	72.1% 27.9%	84.4% 15.6%	78.3% 21.7%

Validation Confusion Matrix

	1	2	
1	7074 36.8%	1463 7.6%	82.9% 17.1%
2	2689 14.0%	7974 41.5%	74.8% 25.2%
	72.5% 27.5%	84.5% 15.5%	78.4% 21.6%

Test Confusion Matrix

	1	2	
1	6802 35.4%	1477 7.7%	82.2% 17.8%
2	2825 14.7%	8096 42.2%	74.1% 25.9%
	70.7% 29.3%	84.6% 15.4%	77.6% 22.4%

All Confusion Matrix

	1	2	
1	46028 36.0%	9960 7.8%	82.2% 17.8%
2	17972 14.0%	54040 42.2%	75.0% 25.0%
	71.9% 28.1%	84.4% 15.6%	78.2% 21.8%

Figure 5.14 **Confusion Matrix of NN Classifier**

The diagonal of each matrix represents the accurate percentage of the data and the total good percentage is located in the blue cells, while the red cells represent the misclassified percentage. As shown in the matrices that the total percentage of the training data is 78.3%, the validation is 78.4%, the testing is 77.6%, and the overall percentage is 78.2%.

51

The accuracy of the classifier did not reach the 100% because of the large number -

128,000 experimental training data of non-defective and defective samples.

Once the training process is done, the classifier is ready for testing any unknown data

that is collected under the same vibrational conditions of the classification data. Table

5.1 shows the results of testing 10 samples, the class of each sample is on the right

side of the table. The Neural Network results is represented in a matrix form. In this

analysis the difference in the third column which represents the average values of the

output is used to recognize the class of data; if the output number of any data under

investigation in the third column is < 0.34 then the sample is non-defective. On the

other hand, if the value is> 0.34 then the sample considered as a defective.

Table 5.1.
Neural Network results

Sample	Output1	Output2	Type
1	0.6717	0.3264	Good
2	0.6705	0.3275	Good
3	0.6649	0.3331	Good
4	0.6692	0.3289	Good
5	0.6989	0.2993	Good
6	0.3158	0.6796	Bad
7	0.3055	0.6897	Bad
8	0.3055	0.6897	Bad
9	0.2969	0.6983	Bad
10	0.2996	0.6956	Bad

The dotted line in Figure 5.16 represent the best validation, while the colored lines are the

classification data. It can be noticed that the classifier did not match the best fit because

of the type of data in which many values are the same for defective and non-defective

samples. The Mean Squared Error (MSE) is the difference between actual and desired

output. The accuracy of the classifier increases when MSE has least value. The values of MSE for best fit is found to be 0.15493 at epoch 383.
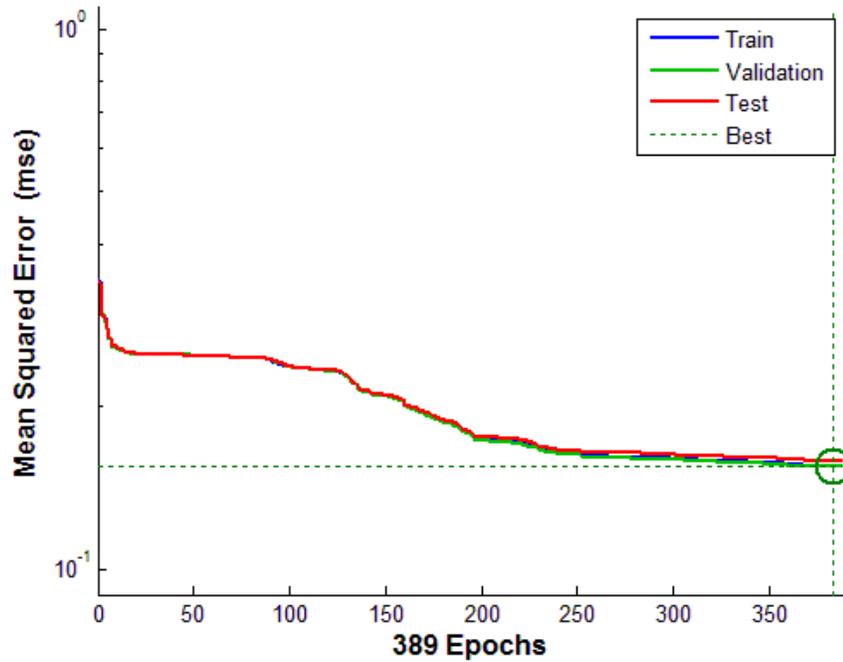

Figure 5.15. **NN Classification Accuracy**

5.4 PSV Frequency Domain Comparison

From the PSV output analyzer for both good and bad samples, a difference could be obtained by observing the location and the values of the peaks.

The data was collected for many samples under different vibrational frequencies and sampling rates. The test was performed on 8 samples at 6400 sampling rate using white noise wave at frequency of 1-5000 HZ. The figures below show the difference between the good and bad under same vibrational conditions. From graphs, at low frequencies the amplitudes of the defective parts have higher values under the same testing conditions.

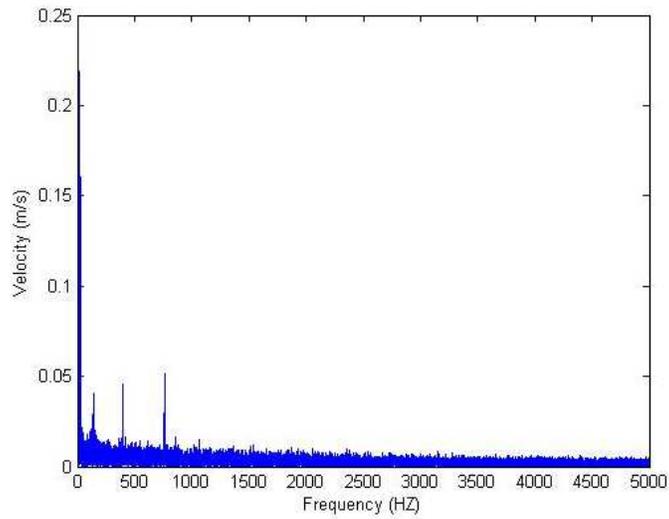*Figure 5.16.* **PSV Non-Defective Sample**
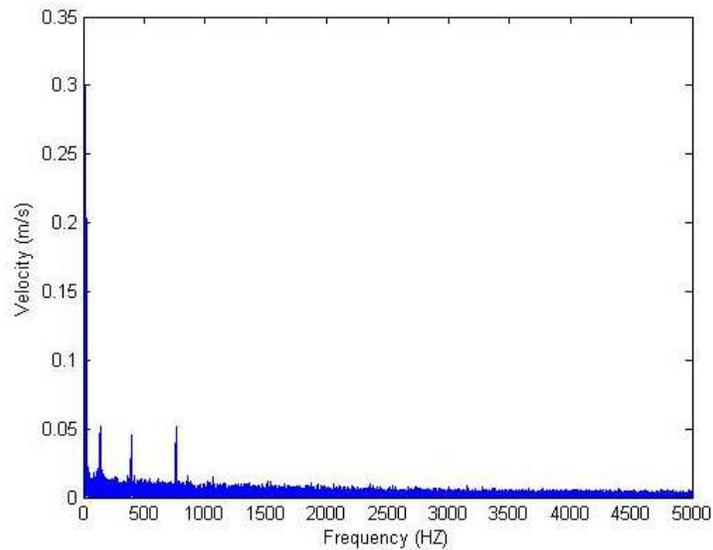
Figure 5.17. **PSV Defective Sample**

According to the frequency experimental results, the defective samples have higher

maximum amplitude of 0.3 m/s when compared to the 0.22 m/s for none defective

samples.

5.4 Hilbert Spectrum

This method is used to analyze the frequency domain data when a non-stationary signal (white noise) is applied.
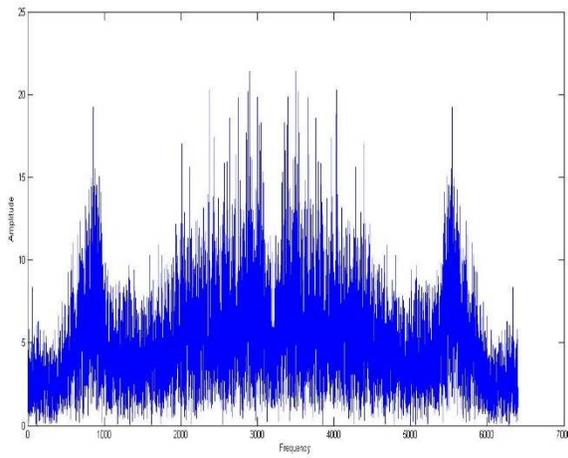
a. Defective
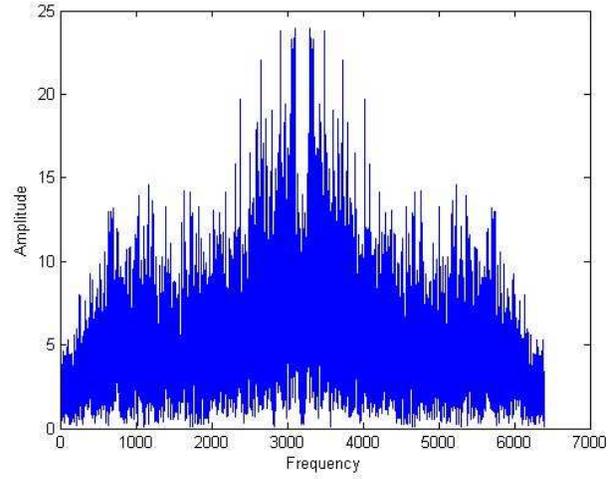
b. Non-Defective

Figure 5.18. **Hilbert Spectrum Results**

a. Defective

b. Non-Defective

Figure 5.19. **IMF Results**

5.5   FEA Modal Response

The model analysis is performed on Non-defective and Defective samples as a "sanity

check". This analysis represents the ideal results of aluminum-6061 cantilever samples.

Two finite element analysis software packages (NASTRAN NX8.0 and ANSYS 13.0) are

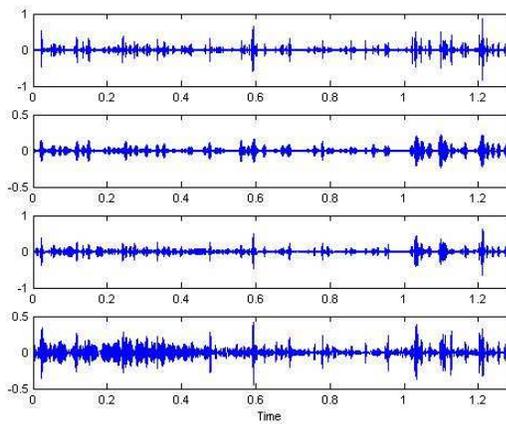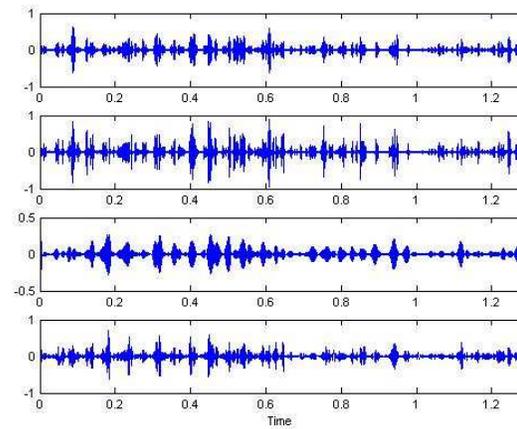employed for this purpose. Tables 5.2 and 5.3 show the natural frequencies in Hertz of

non-defective and defective samples in NASTRAN and ANSYS respectively. From the

results, it can be seen that there is a difference between the samples due to the change in

the stiffness that is caused by the presence of defects. Also the frequencies of the

defective samples are higher than the frequencies of non-defective.

  There are some factor could cause the difference between the FEA packages results

such as the meshing process, software solver, and the applied boundary conditions.

Table 5.2
 NASTRAN results

Non-Defective	Defective
22.90	22.90
143.00	143.00
263.00	281.00
401.00	402.00
624.00	636.00
784.00	785.00
796.00	853.00
1300.00	1300.00
1350.00	1450.00
1930.00	1940.00
1940.00	2110.00
2570.00	2710.00
2700.00	2820.00
3270.00	3590.00
3560.00	3620.00
3580.00	3650.00
4030.00	4480.00

Table 5.3
 ANSYS results

Non-Defective	Defective
22.50	22.50
141.14	140.93
283.20	282.57
396.86	398.73
615.62	617.58
782.99	787.23
860.84	860.57
1305.60	1326.00
1471.50	1473.70
1969.80	2011.30
2135.60	2152.10
2781.40	2875.30
2872.10	2903.70
3532.90	3567.60
3694.20	3763.90
3750.10	3904.70
4625.30	4759.70

| 4550.00 | 4620.00 | | 4873.20 | 5153.90 |
| 4870.00 | 5450.00 | | 5674.70 | 5877.10 |

As shown in the ANSYS results that at low frequencies the non-defective parts have a slightly higher values; this is normally happen because the defects are identified at higher frequencies.

Chapter 6

CONCLUSION

The thesis's main objective was to study the methodologies for NDT using a resonance

testing technique. The testing was performed using a high accuracy Laser Scanner

Vibrometer which generate vibrational signals and acquire data in time and frequency

domain at the same time. To achieve the successful identification/classification, several

pattern recognition, FEA simulation, and system modeling methods were applied. Some

of these methods used time domain data and others uses frequency domain data and.

Based on the analysis and results of each method, it can be noted that-

1. Performing the test in two domains increased the effectiveness of the identification

    process, so if some of the defect signals were not detected in one domain, then they

    could be identified in the other domain.

2. The Modal analysis in ANSYS and NASTRAN NX8.0 represented the ideal case of

    defective and non-defective samples. This analysis provides all the information of the

    natural frequencies and it shows how the values were changing due to the presence of

    the defects especially at high frequency range. There was a small difference between

    the results by ANSYS and NASTRAN NX8.0 that could be attributed to the variation

    in number of the elements, mesh accuracy, and the software solver environment.

3. Fisher's discriminant analysis showed effective results by creating a classification

    border to separate the majority of data values above or under the border. As described

    in sections [4.5.2] and [5.2]. The output of the classifier had two values, each one

    represents a class type. In addition, the defective samples showed higher amplitude

    values and then can be identified easily.

4. Neural Network can be successfully used to identify the class of testing data. However, data training should take place first for generating the class. Second, a validation process should be carried out. Once the training and testing is done to detect the accuracy of classifier on a sample dataset, a testing process should be performed on the actual dataset. The classification results showed the significant difference in the sample's output.

5. The Hilbert Huang Transform (HHT) provided promising results for the time domain data, and then represented it as a frequency spectrum at each IMF. The energy of the spectrum of the none-defective samples is concentrated at 3000 Hz, while for the defective it is at lower frequency value. As illustrated in Figure 5.18, the spread of the amplitudes are different and the defective parts can be easily detected.

6. For the system identification approach, three system Models were predicted using time domain data. Each model described the dynamical behavior of the non-defective samples. The construction of system models was reached by estimating the model's parameters. Based on the final prediction error (FPE) value, the model was selected. The less the value of FPE, led to the best fit model. In this analysis, the Box-Jenkins model showed the least value of (FPE) which is 0.00857601. According to FPE, this model considered as a best fit model to the experimental data that can describe the system dynamical behavior.

7. Estimating the Transfer Function (TF) of any dynamical system is very important because it determines the relationship between the input and the response of the system. The experimental data and the transfer function showed that the system was

under damped and it has a damping ratio<1. The transfer function contained 1 zero and 2 poles.

Based on the results analysis, Neural Network Method seems to have better output than the other methods. The output of the classifier consists of numbers, percentage of well and miss classified data. The difference between the output number of good and bad has an easy criterion of classifying the part as defective or non-defective.

Finally, the Laser Scanning Vibrometer combined with pattern recognition was a successful approach in identifying the defected parts with visible and invisible flaws. This combination could add a crucial advantages to the product's quality control. The future work could include using a micro laser Scanning Vibrometer which is able to detect micro defects and surface flatness. Moreover, a higher frequency vibration is recommended by using the highest range of the scanner (30MHz) in order to get more different amplitudes between the defective and non-defective samples. This recommendation requires a higher frequency range shaker. For better results, it is recommended to use higher quality holding fixture for the samples to represent the ideal cantilever boundary conditions.

REFERENCES

Bishop, C. M. (1995). *Neural Networks for pattern Recognition.* Oxford: CLARENDON PRESS .

Breaban, F., Carlescu, V., Olaro, D., & Gh. Prisacaru, J. C. (2011). Laser Scanning Vibrometry Applied to Non-Destructive Testing of Electro-Acive Polymers. *U.P.B. Sci. Bull.*

Fung, E. H., Wong, Y., Ho, H., & Mignolet, M. P. (2003). Modelling and prediction of machining errors using ARMAX and NARMAX structures. *Applied Mathematical Modeling*.

Hui, L., & Zhang, Y. (2009). Hilbert-Huang transform and marginal spectrum for detection and diagnosis of localized defects in roller bearings. *Journal of Mechanical Science and Technology 23*, 291-301.

Huke, P., Focke, O., Falldorf, C., Kopylow, C. v., & Bergmann, R. B. (2010). Contactless Defect Detection Using Optical Methods for Non Destructive Testing. *NDT in Aerospace*, 8.

Huynh, D., & Tran, D. (2004). *A Non-Destructive Crack Detection Technique Using Vibration Tests.* Structural Integrity and Fracture.

IAEA. (2001). *Guidebook for the Fabrication of Non-Destructive Testing (NDT) Test Specimens.* Vienna: International Atomic Energy.

Jamil, M., Sharkh, S. M., & Hussain, B. (2008). Identification of Dynamic Systems & Selection. In J. M. Arreguin, *Automation and Robotics* (pp. 121-142). Rijeka: I-Tech Education and Publishing.

Kim, D., & Oh, H.-S. (2009). EMD: A Package for Empirical Mode Decomposition and Hilbert Spectrum. *The R Journal* , 40-46.

Li, H., Zhang, Y., & Zheng, H. (n.d.). Hilbert-Huang Transform and Marginal Spectrum for detection and diagnosis of localized defects in roller bearings.

Makridakis, S., & Hibon, M. (n.d.). *ARMA Models and the Box Jenkins Methodology.* Fontainebleau: INSEAD.

Mathworks. (n.d.). *MATLAB*. Retrieved from http://www.mathworks.com/help/econ/box-jenkins-model-selection.html

Ogata, K. (2004). *System Dynamics.* Upper Saddle River: Pearson Education, Inc.

Polytec. (n.d.). *Hardware Manual Polytec Scanning Vibrometer PSV 300.* Retrieved from University Of Cambridge: http://www-mech.eng.cam.ac.uk/dynvib/lab_facilities/vibrometer_hardware_manual.pdf

Price, T. L., Dalley, G., McCullough, P. C., & Choquette, L. (1997). *Manufacturing Advanced Composite Components for Airframes.* National Technical Information Service.

Santulli, C., & Jeronimidis, G. (2006). DEVELOPMENT OF A METHOD FOR NONDESTRUCTIVE TESTING OF FRUITS USING SCANNING LASER VIBROMETRY (SLV). *Jornal of NDT*, 12.

Schwarz, B. J., & Richardson, M. H. (1999). Experimental Modal Analysis. *CSI Reliability Week.* Orlando .

Smith, R. R., Callahan, N., & Strong, S. (2005). Developing a Practical Quality System to Improve Visual Inspections. *Industrial Technology*, 1-7.

Subramanian, D. (2013). *Analysis of Resonance Testing Methodology for Characterization of Parts.* Arizona State University.

Traynor, R. (n.d.). *Non-Contact Vibration Measurement of Micro-Structures.* Retrieved from Lambda Photometric: http://www.lambdaphoto.co.uk/pdfs/DMAC%20Talk%20Warwick%20Uni%208-4-03.pdf

Vanlanduit, S., Guillaume, P., Schoukens, J., & Parloo, E. (2006). *Linear and Nonlinear Damage Detection Using a Scanning Laser Vibrometer.* Brussel.

Vanlanduit, S., Parloo, E., & Guillaume, P. (n.d.). *A Robust Singular Value Decomposition to Detect Damage Under Changing Operating Conditions and Structural Uncertainties.* Brussels.

Wong, F., & Toppings, B. H. (1988). Finite Element Studies For Non-Destructive Vibration Tests. *Comuter and Structures*, 653-669.

Yang, S., & Allen, M. (2012). Output-onlyModalAnalysisusingContinuous-ScanLaserDoppler Vibrometryandapplicationtoa20kWwindturbine. *Mechanical SystemsandSignalProcessing*.